JOURNAL OF MATERIALS SCIENCE 26 (1991) 4621–4625

Magnetic properties of iron-base b.c.c. alloys produced by mechanical alloying

N. KATAOKA, K. SUZUKI*, A. INOUE, T. MASUMOTO
Institute for Materials Research, Tohoku University, Sendai 980, Japan

The structure and magnetic properties of Fe–M (M = Zr, Hf, Co or Si) alloy powders produced by mechanical alloying (MA) of elemental powders or a mixture of elemental powders and alloy powders have been examined. The MA Fe–Zr and Fe–Hf powders have a non-equilibrium b.c.c. phase in the composition range above 90 at% Fe. The coercivity of the MA Fe–Zr and Fe–Hf powders exhibits a minimum value (1300 $A m^{-1}$) combined with a high magnetization of 2.2×10^{-4} $Wb m kg^{-1}$ at 95 at% Fe, which corresponds to the concentration of zero magnetostriction. Although the compacts made from the MA b.c.c. Fe–Zr powders do not exhibit good soft magnetic properties, the permeability of the compacts made from the MA Fe–Co powders annealed at 1173 K for 18 ks in H_2 is nearly the same as that of the alloy ingot produced by conventional casting followed by the same annealing treatment.

1. Introduction

Recently, a number of researches have been carried out on the formation of non-equilibrium phases including an amorphous phase by mechanical alloying (MA) [1–4]. It has been reported [5–14] that MA Fe–Zr alloys have an amorphous state in the composition range of 22 to 70 at % Zr and a supersaturated b.c.c. solid solution in the range to 5 at % Zr, though Zr is insoluble in Fe in an equilibrium solid state [15]. When the glass-formation range in the Fe– Zr system prepared by MA is compared with those prepared by other techniques such as solid-state reaction of multilayers (SSAR), ion-beam mixing of multilayers (IM), liquid quenching (LQ) and vapour quenching (VQ), the range is nearly the same as for IM and SSAR and narrower than for VQ [14, 16].

When one pays attention to advantages due to MA other than the extension of the glass-formation range, MA is also expected to give rise to a new soft magnetic material with a non-equilibrium b.c.c. phase in Fe-based alloys. In particular, soft magnetic materials with a high saturation magnetization and zero magnetostriction have recently been required for the magnetic heads of high-density recording media. As a soft magnetic material to satisfy the requirement, the present authors reported a non-equilibrium b.c.c. Fe-rich alloy film produced by vapour quenching [17, 18].

The aim of this paper is to report the structure and magnetic properties of MA Fe–M (M = Zr, Hf, Co or Si) alloy powders as well as bulk alloys made from the MA powders, in comparison with the data of Fe-based alloys produced by LQ and VQ.

2. Experimental procedure

Powders with a particle size fraction below 150 μm of pure Fe metal and pre-alloyed Fe–M ingots or pure M metal were mixed to give the desired average composition and sealed in a cylindrical stainless steel container under an Ar atmosphere in a glove box. The MA was performed in a planetary ball mill with a ball to a powder weight ratio of 30:1. Since impurities, especially oxygen, exert a significant influence on the alloying behaviour, the concentrations of oxygen and chromium in pure Fe powder were chemically analysed as a function of milling time, as shown in Fig. 1. Although the oxygen and chromium contents tend to increase with increasing milling time, the oxygen content comes mainly from Fe metal powder itself while the chromium content becomes saturated after milling for 1.7×10^5 s. Compacts of the MA powders were produced by hot isostatic pressing (HIP). To improve the soft magnetic properties, the samples were annealed at 573 K under a hydrogen atmosphere before and after HIP.

In addition to the MA samples, ribbons and films of the Fe–Zr system were produced by melt-spinning and r.f. sputtering under argon gas pressure of 3 Pa, respectively. The details of the preparation parameters are described elsewhere [17].

X-ray diffraction patterns were obtained using CuK_α radiation with a graphite monochromator. The 2θ angle was calibrated with Si powder. The saturation magnetization, σ_s, and the coercivity, H_c, at 290 K were measured using a vibrating sample magnetometer in an applied field below 1.2 $MA m^{-1}$ (15 kOe). The relative permeability was measured at 1 kHz using an impedance analyser.

3. Results and discussion

Fig. 2 shows the change of X-ray diffraction pattern as a function of MA time for $Fe_{95}Zr_5$ alloys produced by

*On leave from ALPS Electric Co. Ltd, Nagaoka 940, Japan.

0022–2461/91 $03.00 + .12

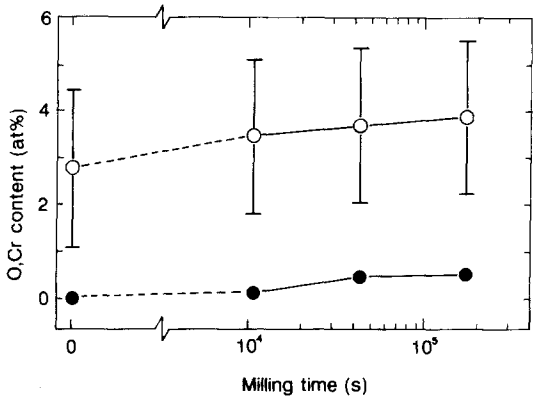

Figure 1 Changes in (○) oxygen and (●) chromium contents in Fe powder with milling time in a stainless steel container.

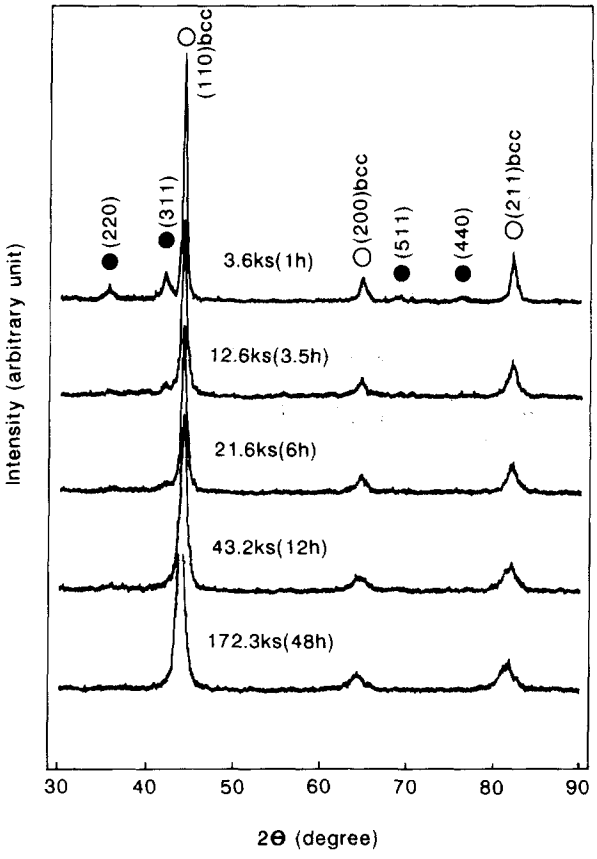

Figure 2 Change in the X-ray diffraction pattern of MA $Fe_{95}Zr_5$ powders with milling time: (○) Fe, (●) Fe_2Zr(C15). (C15 = cubic Laves phase.)

MA of Fe and Fe_2Zr powders. With increasing milling time, the peaks of Fe_2Zr Laves phase disappear and the peaks of the b.c.c. phase shift to the low-angle side accompanied by an increase of their half-width. Fig. 3a shows the lattice parameter of the b.c.c. phase in the MA $Fe_{95}Zr_5$ alloy powders, obtained by X-ray diffraction as a function of milling time. The lattice parameter increases with increasing milling time because of the dissolution of Zr into Fe and becomes saturated after about 100 ks. Accordingly, the subsequent milling time for Fe–Zr alloys was fixed to be 172 ks. The half-width of the b.c.c. (1 1 0) peak for the MA $Fe_{95}Zr_5$ powder as a function of milling time is also shown in Fig. 3b. With an increase of milling time,

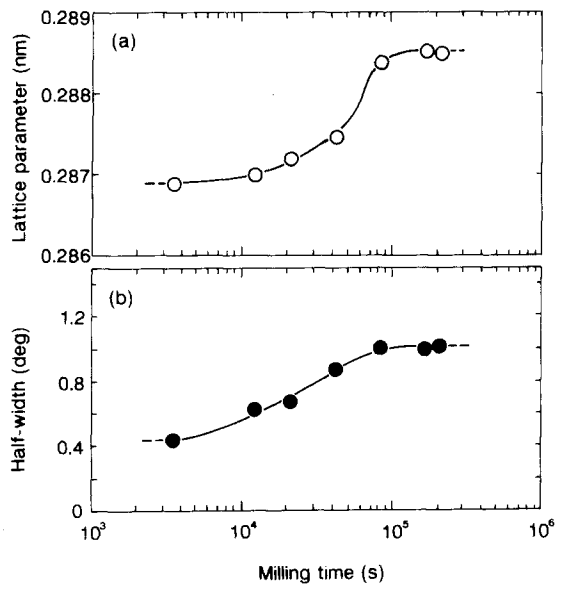

Figure 3 (a) Lattice parameter and (b) half-width of the (1 1 0) peak as a function of milling time for a b.c.c. $Fe_{95}Zr_5$ alloy produced by MA.

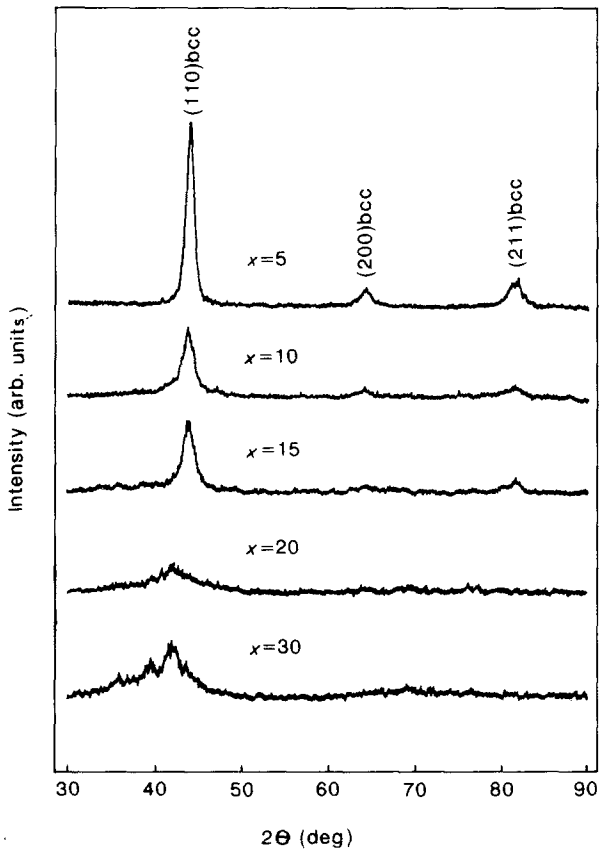

Figure 4 X-ray diffraction patterns of $Fe_{100-x}Zr_x$ alloys (x = 5, 10, 15, 20, 30 at % Zr) milled for 173 ks.

the half-width increases gradually in the range below about 100 ks, probably due to the decrease of grain size and the storing of internal stress, and becomes constant in the milling time range where a constant lattice parameter is obtained.

Fig. 4 shows the X-ray diffraction patterns of $Fe_{100-x}Zr_x$ powders milled for 173 ks. Only b.c.c. peaks are observed for the powders of $x = 5$ and

10 at %, and the peak shape is asymmetric for the $Fe_{85}Zr_{15}$ alloy, suggesting the precipitation of the other phase.

In order to examine the influence of starting materials on the structure and properties of MA $Fe_{100-x}Zr_x$ alloys, either pure Fe and Zr metal powders or pure Fe metal and Fe_2Zr alloy powders were used as the starting materials. Fig. 5a shows the change of the lattice parameter of the b.c.c. phase as a function of Zr content for MA $Fe_{100-x}Zr_x$ alloys made from the two different starting materials. The lattice parameter increases almost linearly with increasing x content because the atomic radius of Zr is larger than that of Fe. In addition, as shown in Fig. 5b, the saturation magnetization at 290 K, σ_s, decreases monotonously with increasing x content. On the other hand, the concentration dependence of the coercivity, H_c, of MA $Fe_{100-x}Zr_x$ alloys is rather complicated as shown in Fig. 5c. Thus, no appreciable difference is seen in the lattice parameter and σ_s for the two kinds of MA $Fe_{100-x}Zr_x$ alloy powders ranging from 0 to 5 at % Zr, while H_C is smaller for the MA Fe–Zr alloys made from Fe and Fe_2Zr than for those made from pure Fe and Zr powders. Accordingly, Fe and pre-alloyed powders were used as the starting materials in the subsequent study.

The lattice parameter, σ_s and H_c of b.c.c. Fe–Zr alloys prepared by the three different methods MA, LQ and VQ are shown as a function of Zr content in Fig. 6. Although the lattice parameter of $Fe_{100-x}Zr_x$ alloys ($x < 10$ at % Zr) increases with increasing x because of the dissolution of Zr with a larger atomic radius, the compositional dependence for the $Fe_{100-x}Zr_x$ alloys produced by MA is similar to that for the VQ alloys and more significant as compared with the LQ alloys. This result suggests that a non-

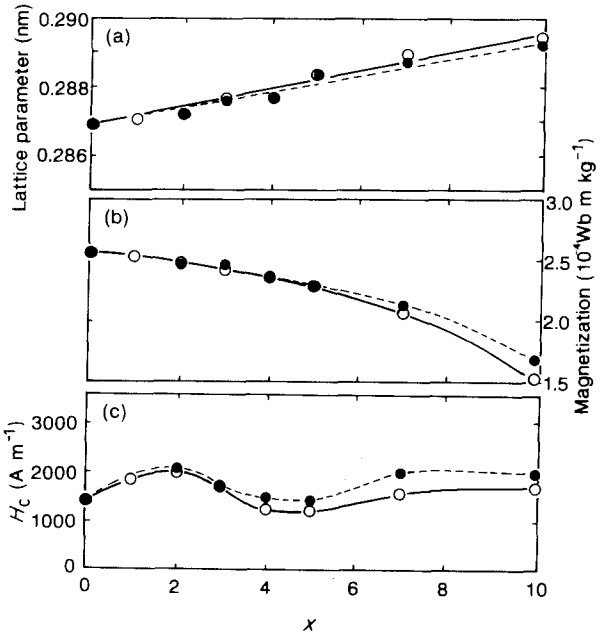

Figure 5 Changes in (a) lattice parameter, (b) magnetization, σ_s, and (c) coercivity, H_c, at 290 K of MA Fe_{100-x} Zr_x alloys (173 ks milling) as a function of Zr content. Data are shown for MA Fe–Zr alloys originating from (○) Fe metal and Fe_2Zr alloy powders and from (●) Fe and Zr metal powders.

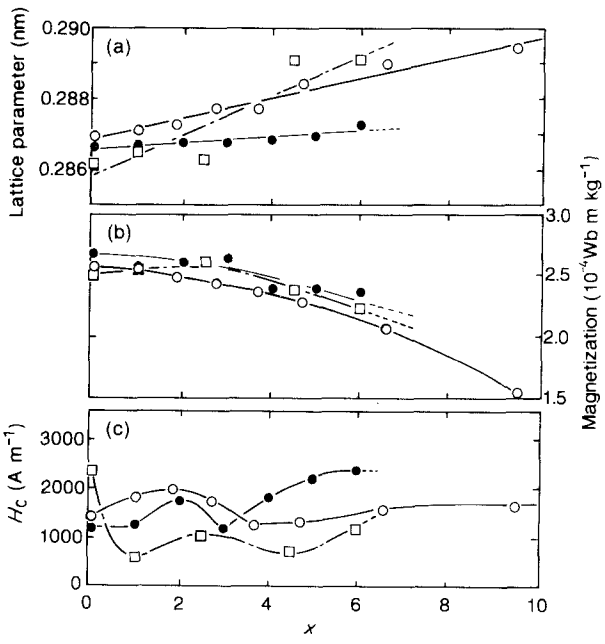

Figure 6 Changes in (a) lattice parameter, (b) σ_s and (c) H_c, at 290 K as a function of Zr content for $Fe_{100-x}Zr_x$ alloys produced by (○) MA (173 ks milling), (●) liquid quenching (LQ) and (□) vapour quenching (VQ).

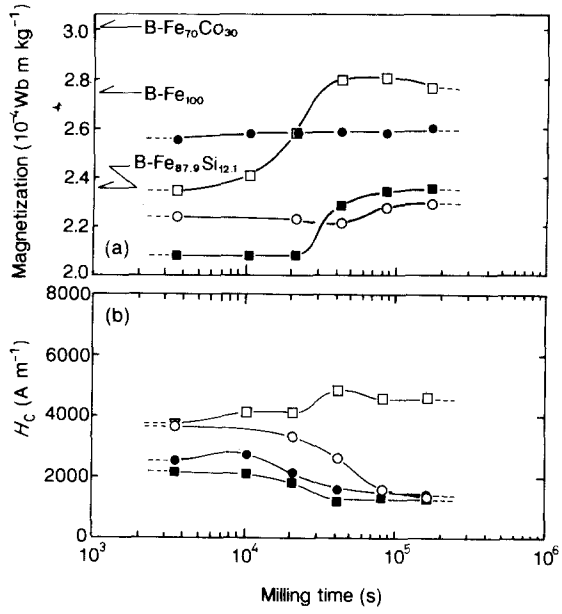

Figure 7 Changes in σ_s and H_c as a function of milling time for MA powders: (●) Fe, (□) $Fe_{70}Co_{30}$, (■) $Fe_{87.9}Si_{12.1}$, (○) $Fe_{95}Zr_5$. The letter B represents the data of the bulk samples.

equilibrium b.c.c. solid solution of Fe–Zr alloys can be produced by MA as well as VQ. The value of σ_s, which is relatively insensitive to microstructure, decreases monotonously with increasing x content and has nearly the same value for the MA, VQ and LQ alloys, as shown in Fig. 6b. In addition, H_c is the smallest for the VQ alloys, suggesting that the VQ method is most useful to produce a non-equilibrium b.c.c. phase with soft magnetic properties.

Fig. 7 shows σ_s and H_c for the MA Fe, $Fe_{70}Co_{30}$, $Fe_{87.9}Si_{12.1}$ and $Fe_{95}Zr_5$ alloys as a function of milling time, along with the data on the σ_s of bulk samples

(marked B). The changes of σ_s and H_c reflect the alloying of Fe and Co, Si or Zr. The change of H_c for Fe may be attributed to a decrease of grain size. Although σ_s for MA $Fe_{87.9}Si_{12.1}$ is nearly the same as that for the bulk sample, σ_s for the MA Fe and $Fe_{70}Co_{30}$ alloys are smaller than those of the bulk samples.

Fig. 8 shows σ_s and H_c as a function of solute content x for $Fe_{100-x}M_x$ (M = Co, Si, Zr or Hf) powders produced by MA for 173 ks. The σ_s values of the bulk samples are also shown for comparison. The H_c of Fe–Zr and Fe–Hf powders exhibits a minimum at 95 at % Fe and a maximum at 85 at % Fe. The minimum has also been observed in VQ Fe–Zr and Fe–Hf alloys [17, 18] and is presumably due to zero magnetostriction. On the other hand, the maximum is due to the coexistence of the b.c.c. and amorphous phases.

Fig. 9 shows the changes in the lattice parameter, a, and H_c of the MA $Fe_{96}Zr_4$ alloy after milling for 173 ks as a function of annealing temperature, T_a. With increasing T_a, the lattice parameter decreases and H_c increases, probably due to the precipitation of other phases. This result suggests that the T_a of MA Fe–Zr powders should be kept below 723 K to improve the soft magnetic properties.

Thermogravimetry of the MA $Fe_{95}Zr_5$ powder was measured at 573 K in a hydrogen atmosphere, as shown in Fig. 10. The weight decreases by 0.6% within an annealing time of 6 ks, suggesting that the oxidized MA powders can be reduced in a hydrogen atmosphere even at a low temperature.

Compacts of the MA powders were produced by HIP and the MA samples were annealed at 573 K under a hydrogen atmosphere before and after HIP to improve the soft magnetic properties. Although the compacts pressed under an applied stress of 196 MPa

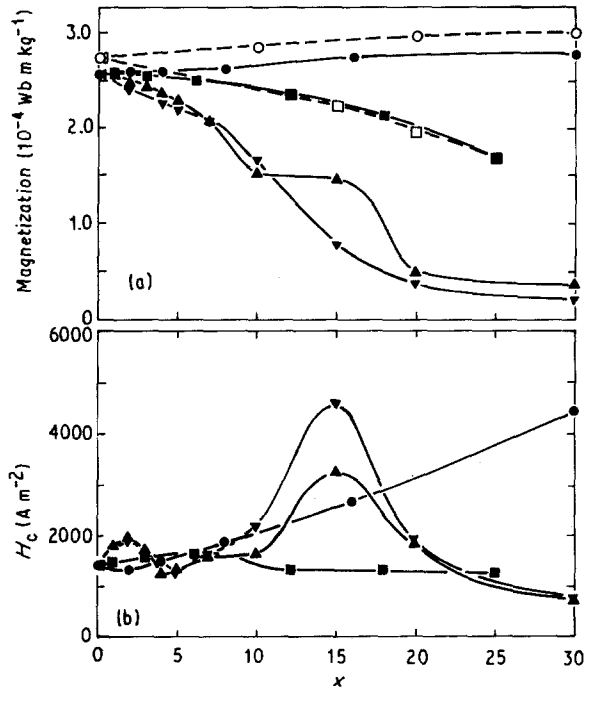

Figure 8 Concentration dependences of σ_s and H_c for $Fe_{100-x}M_x$ powders milled for 173 ks. M = (●) Co, (■) Si, (▲) Zr, (▼) Hf; also bulk samples (○) B-Co, (□) B-Si.

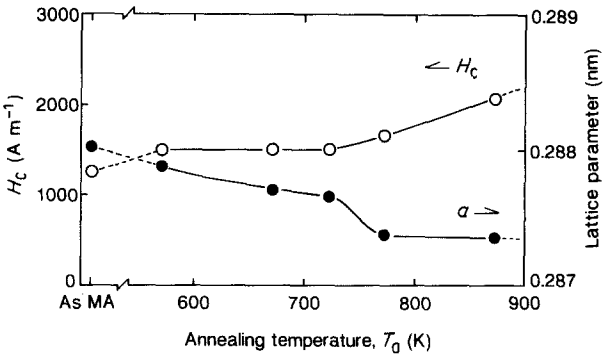

Figure 9 Changes in (●) lattice parameter, a, and (○) H_c of MA $Fe_{96}Zr_4$ alloy powder milled for 173 ks as a function of annealing temperature, T_a; annealing time = 1.8 ks.

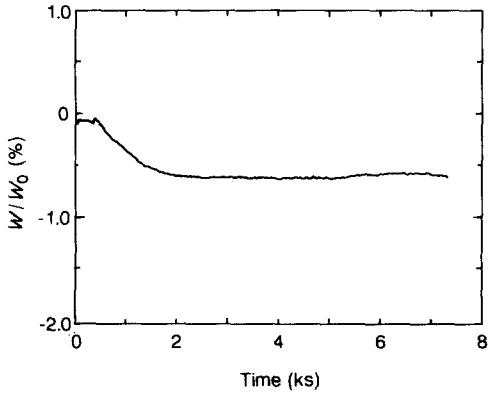

Figure 10 Thermogravimetric curve as a function of annealing time for MA $Fe_{95}Zr_5$ alloy powder milled for 173 ks and annealed at 573 K in a hydrogen atmosphere.

TABLE I The relative effective permeability at 1 kHz for compacts produced by HIP of MA $Fe_{96}Zr_4$ and $Fe_{50}Co_{50}$ powders and an $Fe_{50}Co_{50}$ alloy ingot produced by conventional casting followed by annealing at 573 and 1173 K for 18 ks in a hydrogen atmosphere

Annealing temperature (K)	Relative permeability		
	$Fe_{50}Co_{50}$ (conventional casting)	$Fe_{50}Co_{50}$ (MA → HIP)	$Fe_{96}Zr_4$ (MA → HIP)
573	91	70	55
1173	114	110	–

at 723 K by using MA b.c.c. Fe–Zr powders annealed at 573 K for 18 ks in a hydrogen atmosphere do not exhibit good soft magnetic properties, the permeability of the pressed compacts at 490 MPa and 1073 K made from the MA Fe–Co powders annealed at 1173 K for 18 ks in a hydrogen atmosphere is nearly the same as that for the cast alloy annealed at 1173 K for 18 ks in a hydrogen atmosphere, as shown in Table I.

In conclusion, the non-equilibrium b.c.c. phase in the Fe–Zr and Fe–Hf systems is obtained in the concentration range below 10 at % Zr or Hf by MA and shows a minimum of H_c at 95 at % Fe combined with a high magnetization of 2.2×10^{-4} Wb m kg^{-1}. If the

starting metal powders do not contain any trace of oxygen and the compacts made from the MA powders can be annealed at high temperatures under a hydrogen atmosphere without structural change to an equilibrium phase, the compacts are expected to exhibit good soft magnetic properties.

Acknowledgements

The authors wish to thank Professor H. Fujimori for the magnetic measurements. They also wish to thank Mr M. Hosokawa for his collaboration in the VQ experiment.

References

1. J. S. BENJAMIN, *Met. Trans.* **1** (1970) 2943.
2. A. Y. YERMAKOV, Y. Y. YURCHIKOV and V. A. BARINOV, *Phys. Met. Metall.* **52** (6) (1981) 50.
3. C. C. KOCH, O. B. CAVIN, C. G. McKAMEY and J. O. SCARBROUGH, *Appl. Phys. Lett.* **43** (1983) 1013.
4. W. L. JOHNSON, *Progr. Mater. Sci.* **30** (1986) 81 and references therein.
5. E. HELLSTERN and L. SCHULTZ, *Appl. Phys. Lett.* **48** (1986) 124.
6. *Idem, ibid.* **49** (1986) 1163.
7. C. MICHAELSEN and E. HELLSTERN, *J. Appl. Phys.* **62** (1987) 117.
8. E. HELLSTERN and L. SCHULTZ, *ibid.* **63** (1988) 1408.
9. *Idem, Mater. Sci. Eng.* **97** (1988) 39.
10. W. BIEGEL, H. U. KREBS, C. MICHAELSEN, H. C. FREYHARDT and E. HELLSTERN, *ibid.* **97** (1988) 59.
11. W. KRAUSS, C. POLITIS and P. WEIMAR, *Met. Powder Rep.* **43** (1988) 231.
12. J. ECKERT, L. SCHULTZ and K. URBAN, *J. Less-Common Metals* **145** (1988) 283.
13. G. ENNAS, M. MAGINI, F. PADELLA, P. SUSINI, G. BOFFITTO and G. LICHERI, *J. Mater. Sci.* **24** (1989) 3053.
14. H. U. KREB, *J. Less-Common Metals* **145** (1988) 97.
15. T. B. MASSALSKI, "Binary Alloy Phase Diagrams" (ASM, Ohio, 1986) p. 1125.
16. J. BOTTIGER, K. DYRBYE, K. PAMOUS and R. POULSEN, *Phil. Mag.* **A59** (1989) 569.
17. N. KATAOKA, M. HOSOKAWA, A. INOUE and T. MASUMOTO, *Jpn. J. Appl. Phys.* **28** (1989) L462.
18. *Idem, Mater. Trans., JIM* **31** (1990) 429.

Received 30 April
and accepted 30 November 1990